

Alma Mater Studiorum Università di Bologna
Archivio istituzionale della ricerca

A 14C chronology for the Middle to Upper Palaeolithic transition at Bacho Kiro Cave, Bulgaria

This is the final peer-reviewed author's accepted manuscript (postprint) of the following publication:

Published Version:

Fewlass, H. (2020). A 14C chronology for the Middle to Upper Palaeolithic transition at Bacho Kiro Cave, Bulgaria. NATURE ECOLOGY & EVOLUTION, 4(6), 794-801 [10.1038/s41559-020-1136-3].

Availability:

This version is available at: <https://hdl.handle.net/11585/770560> since: 2022-07-07

Published:

DOI: <http://doi.org/10.1038/s41559-020-1136-3>

Terms of use:

Some rights reserved. The terms and conditions for the reuse of this version of the manuscript are specified in the publishing policy. For all terms of use and more information see the publisher's website.

This item was downloaded from IRIS Università di Bologna (<https://cris.unibo.it/>).
When citing, please refer to the published version.

(Article begins on next page)

This is the final peer-reviewed accepted manuscript of:

Fewlass, H., S. Talamo, L. Wacker, B. Kromer, T. Tuna, Y. Fagault, E. Bard, S. P. McPherron, V. Aldeias, R. Maria, N. L. Martisius, L. Paskulin, Z. Rezek, V. Sinet-Mathiot, S. Sirakova, G. M. Smith, R. Spasov, F. Welker, N. Sirakov, T. Tsanova and J.-J. Hublin (2020). "A 14C chronology for the Middle to Upper Palaeolithic transition at Bacho Kiro Cave, Bulgaria." *Nature Ecology & Evolution* 4(6): 794-801.

The final published version is available online at: 10.1038/s41559-020-1136-3

Rights / License:

The terms and conditions for the reuse of this version of the manuscript are specified in the publishing policy. For all terms of use and more information see the publisher's website.

This item was downloaded from IRIS Università di Bologna (<https://cris.unibo.it/>)

When citing, please refer to the published version.

A ¹⁴C chronology for the Middle–to–Upper Palaeolithic transition at Bacho Kiro Cave, Bulgaria

Fewlass, H.^{1*}, Talamo, S.^{1,2}, Wacker, L.³, Kromer, B.^{1,4}, Tuna, T.⁵, Fagault, Y.⁵, Bard, E.⁵,
McPherron, S. P.¹, Aldeias, V.^{6,1}, Maria, R.¹, Martisius, N. L.⁷, Paskulin, L.⁸, Rezek, Z.^{1,9}, Sinet-
Mathiot, V.¹, Sirakova, S.¹⁰, Smith, G. M.¹, Spasov, R.¹¹, Welker, F.^{12,1}, Sirakov, N.¹⁰, Tsanova, T.¹,
Hublin, J.-J.¹

1) Department of Human Evolution, Max Planck Institute for Evolutionary Anthropology, Leipzig, Germany

2) Department of Chemistry “G. Ciamician”, University of Bologna, Bologna, Italy

3) Ion Beam Physics, ETH Zürich, Zürich, Switzerland

4) Institute of Environmental Physics, University of Heidelberg, Heidelberg, Germany

5) CEREGE, Aix-Marseille University, CNRS, IRD, INRA, Collège de France, Aix-en-Provence, France

6) ICArEHB, University of Algarve, Campus de Gambelas, Faro, Portugal

7) Department of Anthropology, University of California, Davis, USA

8) Department of Archaeology, University of Aberdeen, Aberdeen, Scotland

9) University of Pennsylvania Museum of Archaeology and Anthropology, Philadelphia, PA, USA

10) National Institute of Archaeology and Museum, Bulgarian Academy of Sciences, Sofia, Bulgaria

11) Archaeology Department, New Bulgarian University, Sofia, Bulgaria

12) Evolutionary Genomics Section, Globe Institute, University of Copenhagen, Copenhagen, Denmark.

***Corresponding author:** helen_fewlass@eva.mpg.de

Abstract

The stratigraphy at Bacho Kiro Cave, Bulgaria, spans the Middle to Upper Palaeolithic transition, including an Initial Upper Palaeolithic (IUP) assemblage argued to represent the earliest arrival of Upper Palaeolithic *Homo sapiens* in Europe. We applied the latest techniques in ^{14}C dating to an extensive dataset of newly excavated animal and human bones to produce a robust, high precision radiocarbon chronology for the site. At the base of the stratigraphy, the Middle Palaeolithic (MP) occupation dates to >51,000 BP. A chronological gap of over 3000 years separates the MP occupation from the occupation of the cave by *Homo sapiens*, which extends to 34,000 cal BP. The extensive IUP assemblage, now associated with directly dated *Homo sapiens* fossils at this site, securely dates to 45,820 – 43,650 cal BP (95.4% probability), likely beginning from 46,940 cal BP (95.4% probability). The results provide chronological context for the early occupation of Europe by Upper Palaeolithic *Homo sapiens*.

Introduction

Bacho Kiro Cave in Bulgaria (Fig. 1a) has an archaeological sequence spanning the late Middle Palaeolithic (MP) through the early Upper Palaeolithic. First excavated in 1938¹ and again in 1971-1975², the cave is particularly notable for its distinctive lithic assemblages from Layers 11 and 11a² consisting of elongated Levallois-like blades, retouched points, end-scrapers and splintered pieces, along with pendants made of animal bone and teeth²⁻⁴. A radiocarbon date of >43,000 ^{14}C BP (GrN-7545) (Table 1) on charcoal from Layer 11 made it perhaps one of the earliest Upper Palaeolithic (UP) assemblages in Europe². Originally named 'Bachokirian'², the assemblage is now recognised as part of the Initial Upper Palaeolithic (IUP)^{3,5} and is argued to represent one of the earliest occurrences of Upper Palaeolithic *Homo sapiens* in Europe^{4,6}.

In 2015, the National Archaeological Institute with Museum (NAIM-BAS, Sofia) and the Department of Human Evolution at the Max Planck Institute for Evolutionary Anthropology (MPI-EVA, Leipzig) re-opened the cave with the primary goals of re-sampling the lithic assemblages and re-dating the IUP Layers 11 and 11a⁷. Two excavation sectors adjacent to the area of the 1970s excavations were established (Fig. 1b) and excavated to bedrock. The Main Sector (Fig. 1c) encompasses the sequence as previously described². The Niche 1 is a small and low ceilinged lateral chamber located to the east, preserving only the lower portion of the sequence, including the IUP and underlying Middle Palaeolithic (Fig. 1d). Layer designations were kept separate between these two areas, with the layers from Niche 1 having an “N1-” prefix. The two areas are approximately 4 m apart (Fig. 1b; Extended Data Fig. 1). Previous excavations removed the deposits connecting the two sectors, but field observations of sedimentary characteristics, morphology and archaeological content allow some layers to be correlated (Supplementary Text 1). Here we use the new stratigraphic nomenclature (Fig. 1) wherein Layer 11² corresponds to Layer I in the Main Sector and Layer N1-I in the Niche 1 and Layer 11a² to Layers J and N1-J.

The recent excavations confirm the previously reported stratigraphy and archaeological sequence² (Extended Data Fig. 2). In the Main Sector (Fig. 1c), the stratigraphy begins with the upper part of Layer J, which overlies bedrock and continues through to Layer A0 at the current surface of the cave deposit. The Niche 1 stratigraphy (Fig. 1d) starts with Layer N1-K deposited directly on the bedrock, continuing through Layer N1-J and the distinctive Layer N1-I, into deposits ending with Layer N1-3a. Based on archaeological and geological observations, Layers N1-J, N1-I and N1-H/G in the Niche 1 clearly correspond, respectively, to Layers J, I, and G in the Main sector. The labelling of layers in the upper part of the Niche 1 stratigraphy with numbers (N1-3a-e) reflects the lack of correlation of these layers to lettered layers (A-J) in the Main Sector, although the erosive lower contact of Layers C and N1-3b can be used as a stratigraphic marker in these two areas.

Overall, the sequence is characterised by an exceptionally high artefact density in Layers I and N1-I (15 finds >2 cm per litre of sediment) and low densities in other layers. During the new excavations, we recovered ~14,000 bones and ~2,000 lithics (>2 cm), with >70% of these coming from Layers I and N1-I. These quantities allow the lithic and bone industry to be correlated with previously excavated material and securely characterised as IUP^{2,3} (Supplementary Table 1). In both the old and new lithic collections, the material from Layers J and N1-J is technologically consistent with the Layer I/N1-I assemblage, but the find density is much lower (0.6 finds per litre of sediment). The contact between N1-J and the underlying Layer N1-K is gradual, making the separation between the two sometimes difficult to recognise in the field, and there are some artefacts at the base of N1-J that are consistent with the Middle Palaeolithic assemblage of the underlying Layer N1-K (Levallois flakes from coarse-grained syenite porphyry). In addition to changes in typology and technology from flakes to blades, this transition is marked by a shift in raw material use, from coarser syenite porphyry to fine-grained flint². Layers H—D and N1-H—N1-3a contain no lithic artefacts and a very low density of animal bones. Layers C, B, A2 and A1 in the upper part of the stratigraphy contain characteristic Upper Palaeolithic artefacts, including retouched blades, backed bladelets, carinated end-scrapers, burins, bone tools and pendants. However, their lithic assemblages are poor in diagnostic technological attributes to any particular Upper Palaeolithic industry (Supplementary Table 1).

In the 1980s and 1990s, radiocarbon dating was attempted on material from the 1970s excavation^{2,8}. Although several of the samples produced dates of great antiquity, the sequence of dates was inconsistent with the stratigraphy (Table 1). In particular, a wide range (>43,000 – 34,800 ± 1,150 ¹⁴C BP) was obtained from Layer 11 and a much younger date (33,750 ± 850 ¹⁴C BP) from the underlying Layer 11a. This suggested that either the site was affected by post-depositional mixing between layers, or storage of the material was problematic, and/or that modern carbon contamination had been insufficiently removed from some of the samples prior to ¹⁴C dating, leading to an under-estimation of

their true ages⁸. Since then the establishment of more stringent methods of sample pretreatment, including acid-base-wet oxidation (ABOx) pretreatment for charcoal^{9,10}, and ultrafiltration of bone collagen¹¹⁻¹³, have greatly improved the reliability of radiocarbon dates on Palaeolithic samples¹⁴.

During ZooMS (Zooarchaeology by Mass Spectrometry)¹⁶ screening of a subset of undiagnostic bone fragments from Bacho Kiro Cave, several elements from Layer N1-I (n=4), Layer B (n=1) and from the 1970s collection (Layer B/C; n=1) were identified as hominin⁴. In 2017, a morphologically diagnostic hominin molar was found in Layer J in the Main Sector. DNA analysis confirmed the attribution of these seven elements to *Homo sapiens*. The five newly identified *Homo sapiens* from Layers N1-I and J, described in detail in Hublin *et al.*⁴, are securely associated with the IUP assemblage and represent an early dispersal of *Homo sapiens* into Europe in the Upper Palaeolithic. Given the implications of this assemblage, we sought to establish the range of the IUP at Bacho Kiro Cave and resolve the previous age anomalies by conducting a large-scale dating program. In this paper, we present an extensive dataset of high-precision accelerator mass spectrometer (AMS) radiocarbon dates, which includes direct dating of the newly discovered *Homo sapiens* bones⁴.

Results

We successfully extracted collagen from 139 of the 147 pretreated bones (Supplementary Table 2). The average collagen yield across all layers was 8.3% with several bones in the lowest layers yielding up to 15% (Extended Data Fig. 3), which is much greater than the minimum level of 1% generally required for radiocarbon dating¹⁷ and exceptional for a site of this age range. Isotopic and elemental analysis showed that all collagen extracts are within the range of well-preserved collagen, suitable for ¹⁴C dating¹⁷. Although the C:N values of all extracts (range: 3.0 – 3.4) were within the range of well-preserved collagen, four extracts had C% and N% values slightly above the normal range (marked in red in

Supplementary Table 2), potentially indicating the presence of exogenous material. Only one of these was selected for dating and the age was identical to other bones in close proximity with acceptable C% and N% values. The FTIR spectra of all extracts were characteristic of pure collagen, with no evidence of exogenous material.

It has previously been suggested that the level of deamidation measured in ZooMS analysis could be an efficient pre-screening tool to identify bones with well-preserved collagen for ^{14}C dating¹⁸. The large dataset in this study allowed us to robustly compare deamidation rates of two collagen peptides (P1106 and P1705) with collagen yields following extraction for ^{14}C dating. No correlation was observed between deamidation rates of peptides P1106 and P1705 and collagen yields, indicating that deamidation rates would be an unsuitable method for pre-screening for ^{14}C sampling, at least for Bacho Kiro Cave (Supplementary Text 4; Supplementary Fig. 5).

In total, we AMS dated 95 bones, including 6 *Homo sapiens*. 63% of the dates obtained from animal bones are from specimens that were anthropogenically modified (Fig. 2; Supplementary Text 5). The AMS measurements of the collagen backgrounds which were used in the age correction of all samples were highly reproducible within and between each magazine (~500 mg bone extractions: 2016 mean $F^{14}\text{C}$ =0.00168, SD=0.00018; 2018 mean $F^{14}\text{C}$ =0.00220, SD=0.00025; <100 mg bone extractions: 2018 mean $F^{14}\text{C}$ =0.00291; SD = 0.00034; Supplementary Table 3). Due to the high reproducibility of the background measurements, extended measurement time and high rate of transmission we were able to reach exceptional levels of precision. The finite dates span 49,430 – 27,250 cal BP (95.4% probability; Supplementary Tables 2, 4, 5). Nine of the bones dated beyond the radiocarbon range (>51,000 BP). All of these come from the bottom of the stratigraphic sequence in the Niche 1, from Layer N1-K, the Layer N1-J/K contact, and the lower part of Layer N1-J.

Eleven of the faunal collagen samples were dated in a second AMS lab (MAMS). The radiocarbon dates from the two labs are in statistical agreement for eight of the 11 samples (from Layers C, E, F and N1-I). However, combining dates from the two labs failed for three samples (R-EVA 1735, R-EVA 1737 and R-EVA 1739) from layer N1-I, all dating to >40,000 BP. The reasons for this are not understood so the dates were excluded from further analysis.

Extended Data Figure 4 shows a comparison of the dates from graphite targets (*ca.* 2.5 mg collagen) and the gas ion source (<0.3 mg collagen) of the MICADAS system obtained for hominin bones F6-597 and BK-1653, carried out to cross-check the ages obtained. The level of precision achieved was excellent for both methods, despite a ten-fold reduction in sample size using the gas ion source, and the dates from the different methods measured in two labs are in statistical agreement (Supplementary Table 6), lending reliability to the results.

After Bayesian modelling in OxCal^{19,20}, the agreement index was 80.4 for model 1 (Main Sector), 78.8 for model 2 (Niche 1), both above the generally accepted 60% threshold²¹ (Supplementary Table 5). The high agreement index for the two separate areas indicates that the dates included are in keeping with their stratigraphic positions. The dates from Layers N1-I/I and N1-J/J support the archaeological and geological interpretations that these layers are correlated between the Main Sector and Niche 1. However, the different spatial accumulation of Layer J between the two areas results in a low agreement index ($A_{\text{model}} = 28.9$) for the model combining the dates (Supplementary Fig. 6). We therefore consider the Bayesian models of the two areas separately (Fig. 3; OxCal code in accompanying file).

Discussion

Over the past two decades, the addition of an ultrafiltration step following collagen extraction has shown to be important for removing carbon contamination from Palaeolithic bones¹⁴. The new Bacho Kiro Cave results indicate that several of the 1980s and 1990s dates (Table 1) were affected by carbon contamination, making them appear younger than their actual ages. Our dates resolve the issues of the wide age range previously obtained for Layer I and the young age estimation obtained in Layer J (Table 1).

At the base of the sequence, resting on bedrock, Layer N1-K contains a small (n=82) Middle Palaeolithic assemblage. All five dates from this layer are from *Cervid/Saiga* or *Bos/Bison* (including one with cut-marks) and are >51,000 BP. Overlying Layer N1-K, there are three age clusters represented in Layer N1-J, which accumulated relatively slowly (Supplementary Fig. 4). First, an anthropogenically modified *Ursidae* bone (ETH-86788) and a *Cervid/Saiga* bone (ETH-93195) from the very bottom of Layer N1-J are also >51,000 BP. Second, a minimum of 5,000 ¹⁴C years separates these two dates from the next occupation represented by a cut-marked horse bone (ETH-86787), also excavated from the lower part of Layer N1-J, indicating that hominins were present sometime between 49,430 – 46,940 cal BP (modelled age, 94.5% probability; Fig. 3b). A small number of lithics were recovered from the lower part of Layer N1-J. Some are consistent with the overlying IUP (n=6) and some are consistent with the underlying Middle Palaeolithic (n=8), which is in agreement with the findings of the 1970s excavations². The gradual contact between N1-J and the underlying N1-K makes it difficult to clearly distinguish between the two layers during excavation of this area. From a radiocarbon perspective, it is impossible to know whether the lower part of Layer N1-J relates more to the overlying IUP or more to the underlying Middle Palaeolithic. However, the high resolution of the radiocarbon data suggests temporally distinct occupations in this lower part, which makes an in-situ transition between the Middle Palaeolithic and

181 IUP less likely. The last occupation phase — in the upper part of Layer N1-J — spans from 46,940 –
182 45,130 cal BP (modelled range, 95.4% probability; Fig. 3b) and is associated with a low density of IUP
183 artefacts which share the techno-typological characteristics of those in the overlying Layer N1-I. The
184 dates from Layer J in the Main Sector (Fig. 3a) are at the younger end of the Layer N1-J range (95.4%
185 modelled range: 45,690 – 44,390 cal BP), which supports the geoarchaeological interpretation that only
186 the upper part of this layer is preserved in the Main Sector (where it overlies bedrock and abuts against
187 it towards the south; Supplementary Text 1).

188 The appearance of the IUP in Layer N1-J coincides with a period of climatic warming indicated in various
189 palaeoclimate records across the Northern Hemisphere, including the beginning of Greenland
190 Interstadial 12 (GI12) at $46,950 \pm 1000$ BP in the GICC05 NGRIP ice core²² and beginning at $\sim 47,600$ BP in
191 the Hulu Cave speleothem $\delta^{18}\text{O}$ records in China²³. In closer proximity to Bacho Kiro Cave, mild climatic
192 conditions are indicated in a speleothem $\delta^{13}\text{C}$ record from Ascunsa Cave (AC) in the South Carpathians²⁴
193 (~ 400 km NW of Bacho Kiro Cave) and palaeoclimatic records from the Black Sea^{25,26} and northern
194 Greece²⁷. However, correlations between calibrated ^{14}C dates and palaeoclimate archives linked to
195 calendar ages are limited by the accuracy and precision in the calibration curve²⁸, especially approaching
196 the limit of the method, and in the various palaeoclimate records themselves²⁹. As such these
197 correlations are tentative. Further work on local climatic conditions at Bacho Kiro Cave is on-going and
198 will be discussed further in future.

199 The evidence for the age range of Layer I/N1-I is extremely robust. Twenty-five dates on human remains
200 and anthropogenically modified bones set the modelled age range for the IUP from these correlated
201 layers from 45,820 – 43,650 cal BP (95.4% probability). The radiocarbon dates from the four dated *Homo*
202 *sapiens* bones span the full range of dates coming from anthropogenically modified bones. We chose to
203 focus more on the dating of Layer N1-I in the Niche 1 where this layer is more extensively exposed and

204 more clearly delineated in the stratigraphic sequence. Nevertheless, the four dates from Layer I in the
205 Main Sector fall entirely within the range of Layer N1-I, supporting the archaeological and geological link
206 made between these two areas. The dates from the contact zone I/J in the Main Sector fall within the
207 range of Layer I and the upper part of Layer J. The age ranges from the upper part of Layer N1-J and
208 from Layer N1-I, together with high artefact densities, imply relatively continuous human use of the cave
209 during this interval. The radiocarbon evidence supports the archaeological and geological interpretation
210 that Layer I represents an intensification of the IUP occupation that began during the formation of Layer
211 J.

212 Site formation processes and the low number of artefacts in the layers above Layer I make it difficult to
213 determine when the IUP ended at Bacho Kiro Cave. Layers N1-H, N1-G and G are thick water laid
214 deposits with a low density of artefacts at the base (Layers N1-H and G). These were likely re-deposited
215 from Layer N1-I/I by a stream originating from the cave's inner karst system. These layers essentially
216 seal the underlying Layers N1-K, N1-J/J and N1-I/I⁴. Layers F and E are thick with very low densities of
217 bones and no lithic artefacts. The tight age range from these layers overlap with the youngest age range
218 of Layer I and suggest a rapid rate of sedimentation for Layers G through E. Although no lithics were
219 excavated from Layers F-D during the new excavations, the low density of artefacts recovered during the
220 1970s excavation indicate that the IUP characteristics continue from Layer J to Layer D⁴ (Supplementary
221 Table 1). In the new collection, a relative increase in artefact density occurs in Layer C (42,110 – 36,340
222 cal BP), Layer B (39,000 – 34,970 cal BP) and Layer A2 (35,440 – 34,350 cal BP). The lithic artefacts within
223 these layers are not characteristic of the IUP but rather of various phases of the subsequent Upper
224 Palaeolithic (specifically bladelet production, platforms consistent with the appearance of soft hammer
225 percussion in Layer C, and backed bladelets similar to Gravettian types in Layer A1; Supplementary Table
226 1). In the Main Sector, the Upper Palaeolithic occupation extends to 34,350 cal BP (modelled range) in
227 Layer A2. In Layer A1, the date of 27,610 – 27,250 cal BP (95.4% probability) on a cut-marked *Bos/Bison*

bone (ETH-86796) is consistent with the Gravettian backed bladelets and can be considered the youngest preserved layer. The Dansgaard-Oeschger climatic cycles in the Northern Hemisphere between the end of GI12 and the end of GI8 (~44,000 – 36,500 BP²²) may have been a driver of the demographic turnover seen in archaeological and genetic studies during this interval in Europe^{30,24}, which is indicated at Bacho Kiro Cave by the change in technology seen between the IUP in Layers J and I and the UP forms in Layers C and above.

The Niche 1 has a shorter Upper Palaeolithic sequence than the Main Sector and the same differences in artefact densities. Nevertheless, we attempted to date the layers above Layer N1-I in part to help correlate its stratigraphy to that of the Main Sector. Unlike the rest of the deposits in this area, collagen preservation was very poor in these layers, and only four of the 11 bones had sufficient collagen yields for dating. At least one of the resulting dates (ETH-86776 or ETH-86775) is inconsistent with its stratigraphic position (Supplementary Table 2), and it was not possible to make any connections between the upper layers of the Niche 1 and the Main Sector based on the radiocarbon evidence.

The date of the human bone F6-597 (35,960 – 35,210 cal BP, 95.4% modelled range) from Layer B agrees with the range of dates from the fauna in this layer. The hominin bone BK-1653 identified using ZooMS from the 1970s collection was labelled Layer “6a/7”, which corresponds to the contact of Layers B and C in the new excavation. This bone was excluded from the modelling because of uncertainties over its exact stratigraphic context, but its age (34,810 – 34,210 cal BP, 95.4% probability) fits with the dates on fauna from Layer A2. Both human bones from the Upper Palaeolithic levels of the site (BK-1653 and F6-597) were dated using both the gas ion source and graphite methods to cross check the obtained ages (Extended Data Fig. 4; Supplementary Table 6). The high level of agreement between the two methods measured in two different AMS laboratories serves as further evidence of the suitability of the gas ion source of the MICADAS for dating precious and/or small archaeological bone samples^{31,32}.

Conclusion

The chronology presented here for Bacho Kiro Cave constitutes an extensive set of high-quality collagen samples radiocarbon dated at exceptional precision. To the best of our knowledge, this study represents one of the largest ^{14}C datasets from a single Palaeolithic site processed by one team. This large effort was made to resolve the questions left open by the previous dates from this eponymous site. The integrity of the stratigraphic sequence is clearly indicated by the dates. The extensive dataset allows us to securely place the IUP from correlated Layers I and N1-I in the interval from 45,820 – 43,650 cal BP (95.4% probability). The start date for the IUP at Bacho Kiro Cave falls during the accumulation of Layer N1-J, likely from 46,940 cal BP (95.4% probability). Direct radiocarbon dating of the four *Homo sapiens* bones from Layer N1-I confirms their association with the IUP assemblage, and represents the earliest direct evidence of our species in Europe in the Upper Palaeolithic.

Even as the precision of AMS measurements increases, one of the constraints of dating samples so close to the limit of the ^{14}C method is the imprecision of the calibration curve in this time range. The output of the Bayesian modelling presented here may change as the resolution of the calibration curve improves^{23,33,34}. On-going work in this area is crucial for enhancing our understanding of the timing of major events in hominin adaptations and demographic processes during this time period.

Materials and Methods

Sample selection for radiocarbon dating

Bones were selected for radiocarbon dating from finds excavated during the 2015-2017 field seasons spanning the stratigraphy in both the Main Sector (Supplementary Figs. 1-2) and the Niche 1 (Supplementary Figs. 3-4). In total, 141 animal and 6 hominin bones were selected for collagen extraction (Supplementary Table 2). Where possible, animal bones that had signs of anthropogenic

modification (cut-marks, impact fractures) on their surfaces were selected (53% of the sample set) (Fig. 2). A particular focus was given to sampling the IUP in Layer N1-I, where the layer was extensively exposed. Due to the exceptionally high density of bone in this layer (Supplementary Fig. 4), we were able to select a high number of bones (77%) with anthropogenic modifications. A small number of samples were also taken from Layer I in the Main Sector to confirm the stratigraphic link between the two areas through radiocarbon dating. During excavation of the contact zone between Layers I and J in the Main Sector, precise attribution of the finds to either Layer I or J was sometimes impossible to make, due to the sediment moistness and the presence of large limestone rubble. These finds are labelled as “I/J” to indicate that they come from the contact zone between these two layers.

Bone pretreatment

The bones were pretreated in the Department of Human Evolution at the MPI-EVA, following the collagen extraction plus ultrafiltration protocol described in Fewlass et al³¹ (see Supplementary Text 2 for further details). To preserve as much material as possible for aDNA and palaeoproteomic analysis, small aliquots of the hominin bones were sampled (80-110 mg) for direct ¹⁴C dating. The quality of all the collagen extracts was assessed based on collagen yield, elemental (C%, N%, C:N) and stable isotopic values ($\delta^{13}\text{C}$, $\delta^{15}\text{N}$)¹⁷. All collagen extracts were analysed with Fourier transformed infra-red (FTIR) spectroscopy prior to dating to look for evidence of incomplete demineralisation, degraded collagen or the presence of any exogenous material in the extracts³⁵⁻³⁷.

AMS measurement

Collagen extracts from 6 human bones and 89 animal bones and teeth were selected for radiocarbon dating based on stratigraphic position, signs of anthropogenic surface modification and the level of collagen preservation (Supplementary Table 2). The collagen extracts were graphitised using the AGE III³⁸ and dated using the MICADAS³⁹ in the Laboratory of Ion Beam Physics at ETH Zürich, Switzerland

(lab code: ETH). The latest model of the MICADAS, equipped with Helium stripping gas⁴⁰ and permanent magnets⁴¹, has been in operation at ETH Zürich since the beginning of 2016 and produced high ion currents, a high rate of transmission, and a low and stable instrument background (~53,000 ¹⁴C BP). Oxalic Acid II standards and collagen backgrounds extracted alongside the samples were measured in the same magazine and used in the age calculation (AMS determinations of collagen and instrument backgrounds are included in Supplementary Table 3). Data reduction was performed using BATS software⁴². An additional 1‰ was added to the error calculation of the samples, as per standard practice.

Several collagen samples were split and dated in a second AMS lab to cross check the measurements. Eleven fauna collagen samples plus collagen extraction backgrounds were weighed into cleaned tin cups and sent to the Klaus-Tschira-AMS facility in Mannheim, Germany (lab code: MAMS), where they were catalytically converted to graphite and dated with the MICADAS-AMS⁴³. Here, data reduction was also carried out using BATS software⁴², and errors were calculated from the blanks and standards measured in the same magazine. An additional 1‰ was included in the final error calculation, as per the standard practice at MAMS.

In addition to graphitisation and AMS measurement at ETH Zürich, small aliquots of collagen (<100 µg C) from *Homo sapiens* bones F6-597 and BK-1653 were measured using the gas ion source of the AixMICADAS^{40,31-32} following the protocol described in Fewlass et al³².

Calibration and Bayesian modelling

Calibration and Bayesian chronological analysis was performed against the IntCal13 dataset²⁰ using OxCal 4.3¹⁹. Where multiple measurements were made from the same collagen extract, the R_Combine function in OxCal 4.3¹⁹ was used to combine them. As part of this function, a chi-squared (χ^2) test is performed to see if the dates are in statistical agreement⁴⁴.

Some of the dates were excluded from the Bayesian chronological analysis: nine dating beyond 51,000 BP; four from the upper N1-3 layers; ten from the Layer I/J contact zone; three from Layer N1-I which failed the χ^2 test; one (ETH-71326) which was identified post-excavation as originating from next to the 1970s backfill; and the human bone (BK-1751) recovered from the 1970s collection as the context is not certain (Supplementary Table 2). Outlier analysis was performed for the rest of the dataset (n=67) so that outliers could be manually eliminated²¹. Each layer was assigned a phase, and we used a general outlier model with prior outlier probabilities set to 0.05²¹. As OxCal compresses posterior date distributions around the most precise date within a phase, the ordering of the data within each phase does not affect the model outcome so the dates were ordered chronologically rather than by stratigraphic depth. Dates from the Main Sector (model 1) and Niche 1 (model 2) were first considered separately. As Layers I and J have been archaeologically and geologically correlated between the two areas, the dates were then combined in a third model (model 3). The likelihood of individual dates being outliers was considered based on their depositional histories, posterior outlier probabilities and individual agreement indices (<60% indicates the date could be incompatible with the model²¹) in the three models. Based on this information, 14 of the 67 dates (shown in red in Supplementary Table 4 and discussed in Supplementary Text 6) were identified as outliers. When the dates from the two areas were combined (model 3), a higher number of dates were identified as outliers but only those identified as outliers in the individual models were excluded from the final model. All models were then run again without outlier analysis with the spurious dates removed and were assessed based on the model agreement indices²¹ (Supplementary Table 5).

ZooMS collagen fingerprinting

All specimens (n=147) in the radiocarbon study were also analysed using MALDI-TOF-MS collagen peptide mass fingerprinting^{16,45} in order to provide accurate species identifications for each specimen (Supplementary Text 3).

Data Availability

All data is available in the manuscript and supplementary materials.

Code Availability

OxCal script is included in the supplementary information.

References

- 1 Garrod, D., Howe, B. & Gaul, J. Excavations in the cave of Bacho Kiro, north-east Bulgaria. *Bulletin of the American School of Prehistoric research* **15**, 46-76 (1939).
- 2 Kozłowski, J. K. *Excavation in the Bacho Kiro cave (Bulgaria): Final Report*. (Państwowe Wydawnictwo Naukowe, 1982).
- 3 Tsanova, T. *Les Débuts du Paléolithique Supérieur dans l'Est des Balkans. Réflexion à Partir de l'Étude Taphonomique et Techno-Économique des Ensembles Lithiques de Bacho Kiro (Couche 11), Temnata (Couches VI et 4) et Kozarnika (Niveau VII)* Vol. 1752 (BAR International Series, 2008).
- 4 Hublin, J. J. *et al.* Initial Upper Palaeolithic *Homo sapiens* remains from Bacho Kiro Cave (Bulgaria) *Nature* (Submitted).
- 5 Kuhn, S. L. & Zwyns, N. Rethinking the Initial Upper Paleolithic. *Quaternary International* **347**, 29-38, doi:10.1016/j.quaint.2014.05.040 (2014).
- 6 Hublin, J. J. The modern human colonization of western Eurasia: when and where? *Quaternary Science Reviews* **118**, 194-210, doi:10.1016/j.quascirev.2014.08.011 (2015).
- 7 Sirakov, N. *et al.* Reopened Bacho Kiro - new data on Middle/Upper Palaeolithic transition and Early-Middle stages of Upper Palaeolithic. (Bulgarian Academy of Sciences, Sofia, 2017).
- 8 Hedges, R. E. M., Housley, R. A., Bronk Ramsey, C. & Van Klinken, G. J. Radiocarbon dates from the Oxford AMS system: Archaeometry datelist 18. *Archaeometry* **36**, 337-374, doi:10.1111/j.1475-4754.1994.tb00975.x (1994).
- 9 Bird, M. *et al.* Radiocarbon dating of "old" charcoal using a wet oxidation, stepped-combustion procedure. *Radiocarbon* **41**, 127-140 (1999).
- 10 Wood, R. E. *et al.* Testing the ABOx-SC method: dating known-age charcoals associated with the Campanian Ignimbrite. *Quaternary Geochronology* **9**, 16-26, doi:10.1016/j.quageo.2012.02.003 (2012).
- 11 Brown, T. A., Nelson, D. E., Vogel, J. S. & Southon, J. R. Improved collagen extraction by modified Longin method. *Radiocarbon* **30**, 171-177 (1988).
- 12 Bronk Ramsey, C., Higham, T., Bowles, A. & Hedges, R. Improvements to the pretreatment of bone at Oxford. *Radiocarbon* **46**, 155-164 (2004).
- 13 Talamo, S. & Richards, M. A comparison of bone pretreatment methods for AMS dating of samples >30,000 BP. *Radiocarbon* **53**, 443-449 (2011).
- 14 Higham, T. European Middle and Upper Palaeolithic radiocarbon dates are often older than they look: problems with previous dates and some remedies. *Antiquity* **85**, 235-249 (2011).
- 15 Evin, J., Marien, G. & Pachiadi, C. Lyon natural radiocarbon measurements VII. *Radiocarbon* **20**, 19-57 (1978).
- 16 Buckley, M., Collins, M., Thomas-Oates, J. & Wilson, J. C. Species identification by analysis of bone collagen using matrix-assisted laser desorption/ionisation time-of-flight mass

spectrometry. *Rapid Communications in Mass Spectrometry* **23**, 3843-3854, doi:10.1002/rcm.4316 (2009).

17 van Klinken, G. J. Bone collagen quality indicators for palaeodietary and radiocarbon measurements. *Journal of Archaeological Science* **26**, 687–695 (1999).

18 Wilson, J., van Doorn, N. L. & Collins, M. J. Assessing the extent of bone degradation using glutamine deamidation in collagen. *Analytical Chemistry* **84**, 9041-9048, doi:10.1021/ac301333t (2012).

19 Bronk Ramsey, C. Bayesian analysis of radiocarbon dates. *Radiocarbon* **51**, 337-360 (2009).

20 Reimer, P. J. *et al.* IntCal13 and Marine13 radiocarbon age calibration curves 0–50,000 years cal BP. *Radiocarbon* **55**, 1869–1887 (2013).

21 Bronk Ramsey, C. Dealing with outliers and offsets in radiocarbon dating. *Radiocarbon* **51**, 1023-1045 (2009).

22 Svensson, A. *et al.* A 60 000 year Greenland stratigraphic ice core chronology. *Climate of the Past* **4**, 47-57 (2008).

23 Cheng, H. *et al.* Atmospheric $^{14}\text{C}/^{12}\text{C}$ changes during the last glacial period from Hulu Cave. *Science* **362**, 1293-1297, doi:10.1126/science.aau0747 (2018).

24 Staubwasser, M. *et al.* Impact of climate change on the transition of Neanderthals to modern humans in Europe. *Proceedings of the National Academy of Sciences* **115**, 9116-9121, doi:10.1073/pnas.1808647115 (2018).

25 Nowaczyk, N. R., Arz, H. W., Frank, U., Kind, J. & Plessen, B. Dynamics of the Laschamp geomagnetic excursion from Black Sea sediments. *Earth and Planetary Science Letters* **351-352**, 54-69, doi:10.1016/j.epsl.2012.06.050 (2012).

26 Wegwerth, A. *et al.* Black Sea temperature response to glacial millennial-scale climate variability. *Geophysical Research Letters* **42**, 8147-8154, doi:10.1002/2015gl065499 (2015).

27 Müller, U. C. *et al.* The role of climate in the spread of modern humans into Europe. *Quaternary Science Reviews* **30**, 273-279, doi:10.1016/j.quascirev.2010.11.016 (2011).

28 Giaccio, B., Hajdas, I., Isaia, R., Deino, A. & Nomade, S. High-precision ^{14}C and $^{40}\text{Ar}/^{39}\text{Ar}$ dating of the Campanian Ignimbrite (Y-5) reconciles the time-scales of climatic-cultural processes at 40 ka. *Scientific Reports* **7**, 45940, doi:10.1038/srep45940 (2017).

29 Buizert, C. *et al.* Abrupt ice-age shifts in southern westerly winds and Antarctic climate forced from the north. *Nature* **563**, 681-685, doi:10.1038/s41586-018-0727-5 (2018).

30 Fu, Q. *et al.* The genetic history of Ice Age Europe. *Nature* **534**, 200-205, doi:10.1038/nature17993 (2016).

31 Fewlass, H. *et al.* Size matters: radiocarbon dates of <200 µg ancient collagen samples with AixMICADAS and its gas ion source. *Radiocarbon* **60**, 425-439, doi:10.1017/rdc.2017.98 (2017).

32 Fewlass, H. *et al.* Pretreatment and gaseous radiocarbon dating of 40–100 mg archaeological bone. *Scientific Reports* **9**, 5342, doi:10.1038/s41598-019-41557-8 (2019).

33 Talamo, S. *et al.* RESOLUTION: Radiocarbon, tree rings, and solar variability provide the accurate time scale for human evolution, presented at: *7th Annual Meeting of the European Society for the Study of Human Evolution*. Abstract in: PESHE, Vol. 6, 194 (Leiden, The Netherlands, 2017).

34 Reimer, P. J. *et al.* A preview of the IntCal19 radiocarbon calibration curves, presented at: *23rd International Radiocarbon conference* (Trondheim, Norway, 2018).

35 DeNiro, M. J. & Weiner, S. Chemical, enzymatic and spectroscopic characterization of “collagen” and other organic fractions from prehistoric bones. *Geochimica et Cosmochimica Acta* **52**, 2197-2206, doi:10.1016/0016-7037(88)90122-6 (1988).

36 Yizhaq, M. *et al.* Quality controlled radiocarbon dating of bones and charcoal from the early pre-pottery Neolithic B (PPNB) of Motza (Israel). *Radiocarbon* **47**, 193-206, doi:10.1017/S003382220001969X (2005).

- 37 D'Elia, M. *et al.* Evaluation of possible contamination sources in the ^{14}C analysis of bone samples by FTIR spectroscopy. *Radiocarbon* **49**, 201-210 (2007).
- 38 Wacker, L., Němec, M. & Bourquin, J. A revolutionary graphitisation system: fully automated, compact and simple. *Nuclear Instruments and Methods in Physics Research Section B: Beam Interactions with Materials and Atoms* **268**, 931-934, doi:10.1016/j.nimb.2009.10.067 (2010).
- 39 Wacker, L. *et al.* MICADAS: routine and high-precision radiocarbon dating. *Radiocarbon* **52**, 252–262 (2010).
- 40 Bard, E. *et al.* AixMICADAS, the accelerator mass spectrometer dedicated to ^{14}C recently installed in Aix-en-Provence, France. *Nuclear Instruments and Methods in Physics Research Section B: Beam Interactions with Materials and Atoms* **361**, 80-86, doi:10.1016/j.nimb.2015.01.075 (2015).
- 41 Salehpour, M., Håkansson, K., Possnert, G., Wacker, L. & Synal, H. A. Performance report for the low energy compact radiocarbon accelerator mass spectrometer at Uppsala University. *Nuclear Instruments and Methods in Physics Research Section B: Beam Interactions with Materials and Atoms* **371**, 360-364, doi:10.1016/j.nimb.2015.10.034 (2016).
- 42 Wacker, L., Christl, M. & Synal, H. A. Bats: a new tool for AMS data reduction. *Nuclear Instruments and Methods in Physics Research Section B: Beam Interactions with Materials and Atoms* **268**, 976-979, doi:10.1016/j.nimb.2009.10.078 (2010).
- 43 Kromer, B., Lindauer, S., Synal, H. A. & Wacker, L. MAMS - A new AMS facility at the Curt-Engelhorn-Centre for Archaeometry, Mannheim, Germany. *Nuclear Instruments and Methods in Physics Research Section B: Beam Interactions with Materials and Atoms* **294**, 11-13, doi:10.1016/j.nimb.2012.01.015 (2013).
- 44 Ward, G. K. & Wilson, S. R. Procedures for comparing and combining radiocarbon age determinations: a critique. *Archaeometry* **20**, 19-31, doi:10.1111/j.1475-4754.1978.tb00208.x (1978).
- 45 Welker, F. *et al.* Palaeoproteomic evidence identifies archaic hominins associated with the Châtelperronian at the Grotte du Renne. *Proceedings of the National Academy of Sciences* **113**, 11162 (2016).

Acknowledgements

The re-excavation of Bacho Kiro Cave is a joint project between the National Institute of Archaeology and Museum, Bulgarian Academy of Sciences, Sofia and the Human Evolution department of the Max Planck Institute for Evolutionary Anthropology, Leipzig. This work was funded by the Max Planck Society. Graphitisation and AMS dating in Switzerland were funded by ETH Zürich. The AixMICADAS and its operation are funded by the Collège de France and the EQUIPEX ASTER-CEREGE (PI E.B.). The authors acknowledge the vital contribution of all the excavators who have worked at Bacho Kiro Cave since 2015.

Author contributions

The study was devised by J.-J.H, S.T., S.M., Ts.Ts, N.S. and H.F. Archaeological excavation was undertaken by Ts.Ts., N.S., Z.R., V.A. and S.M., who all contributed contextual information. The excavation lab and collection was organised by V.S.-M. Lithic analysis was performed by Ts.Ts., N.S., S.S. and S.M. Zooarchaeological analysis was performed by G.S. and R.S. N.M. classified the bone tools in the sample set. Stratigraphic and micromorphological analysis was carried out by V.A. ZooMS was carried out by F.W., L.P. and V.S.-M. Sample pretreatment and EA-IRMS analyses were carried out by H.F. FTIR analyses were carried out by H.F. and R.M. Graphitisation and AMS dating at ETH Zürich was carried out by L.W.,

B.K. and H.F. Dating with the AixMICADAS was carried out by E.B., Y.F. and Th.T. Bayesian modelling was carried out by H.F. and S.T. H.F. wrote the paper with input from all authors.

Competing Interests

The authors declare no competing interests.

Additional information

Supplementary information for this paper is available at XXX. Note that Supplementary Tables 2 - 5 are included as separate sheets in the accompanying supplementary Excel file.

Figure Legends

Figure 1. Bacho Kiro Cave: **a)** location of the cave in Bulgaria, Balkan Peninsula, south-eastern Europe (base map from naturalearthdata.com); **b)** site plan showing the location of excavations carried out in 1971-1975 (centre, light orange) and the new excavations, in the Main Sector (top) and in the Niche 1 (left). The locations of the profiles shown in c-d are marked by red lines; **c)** stratigraphic sequence in the Main Sector, along squares G5 and G6 in 2015. Note the presence of Layer J overlying the bedrock at the bottom of the sequence; **d)** Extract from a 3D model of Niche 1, showing the stratigraphic sequence. Layer attributions from this sector have an 'N1-' prefix. Note the distinctive dark colour of Layer N1-I. In c and d, numbers in white squares show the layer attributions from the 1970s excavations. Letters in white circles show the layer attributions from the recent excavations.

Figure 2. A selection of bone specimens from Bacho Kiro Cave with human bone surface modification that were radiocarbon dated in this study: **a)** *Equidae* bone (R-EVA 2298/CC7-2607) from the lower part of Layer N1-J with cut-marks (ETH-86787: $44,890 \pm 450$ ^{14}C BP); **b)** *Ursidae* bone (R-EVA 2290/BB8-207) from Layer N1-I with a large impact fracture scar, scrape marks and marks consistent with use as a retoucher (ETH-86783: $40,340 \pm 280$ ^{14}C BP); **c)** *Bos/Bison* rib (R-EVA 2352/F5-182) from the contact zone

between Layers I and J in the Main Sector with parallel cut-marks (ETH-86813: $40,160 \pm 270$ ^{14}C BP); **d)** *Bos/Bison* long bone (R-EVA 2333/F5-107) excavated from Layer I used as a retoucher (ETH-86808: $41,350 \pm 310$ ^{14}C BP); **e)** *Bos/Bison* long bone (R-EVA 2311/CC7-2750) from layer N1-K with cut-marks (ETH-86793: $>51,000$ ^{14}C BP). Scale bar is 5 cm.

Figure 3. Bayesian chronological models for Bacho Kiro Cave of material excavated during the 2015-2017 field seasons from the **a)** Main Sector (model 1) and **b)** Niche 1 (model 2). The AMS lab numbers are shown on the left side. The dates were calibrated against the IntCal13 dataset²⁰, and the modelling was performed in OxCal 4.3¹⁹. Where more than one measurement was made from the same collagen extract, dates were combined (R_Combine) in OxCal 4.3. **The distributions of dates from the Niche 1 are shown in green and from the Main Sector in black. The dates from the *Homo sapiens* bones from Layer N1-I and Layer B are shown in purple.** The radiocarbon likelihoods of calibrated dates (without modelling) are shown in the lighter shade and the posterior distributions (after modelling) are darkly shaded. Brackets show the 68.2% and 95.4% probability ranges of the calibrated dates. Dates marked with an asterisk (*) are from bones bearing signs of anthropogenic modification. Note that 2 further dates from the bottom of Layer N1-J date to $>51,000$ BP (beyond model range) as do 2 dates from the N1-J/K contact and 5 dates from the underlying Layer N1-K. Further information is included in Supplementary Tables 2, 4 and 5. OxCal code is included in Supplementary Text 7.

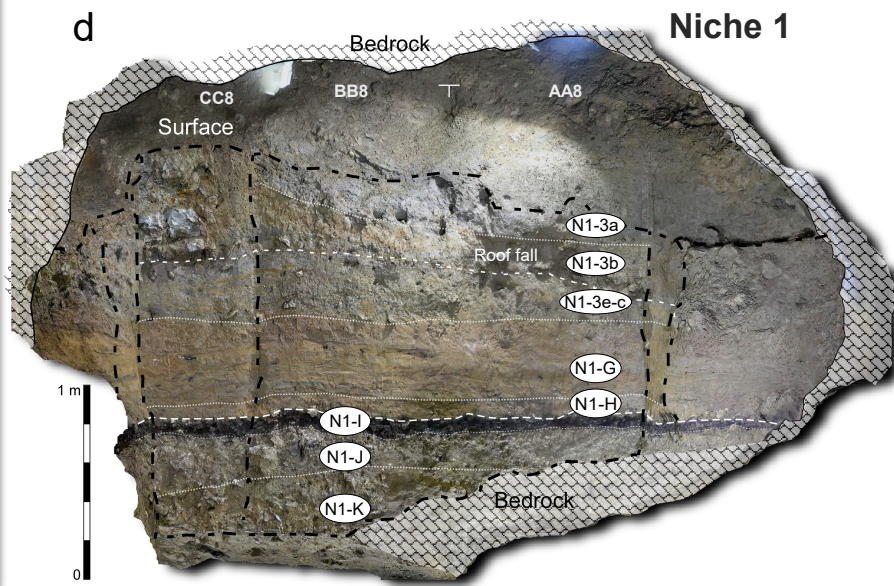
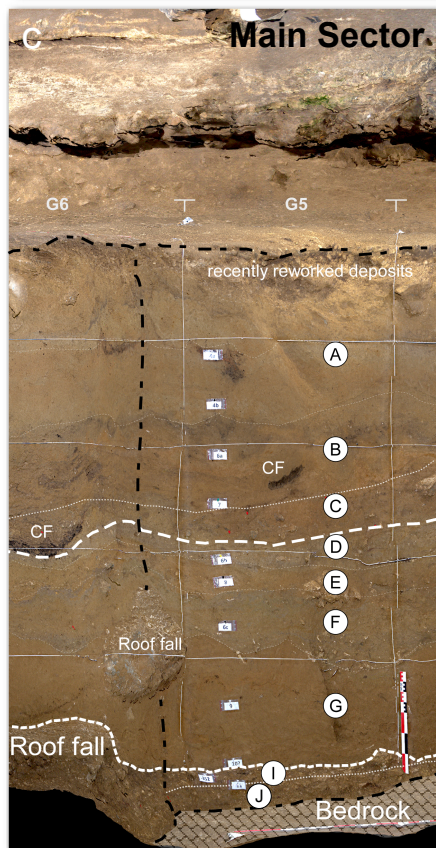
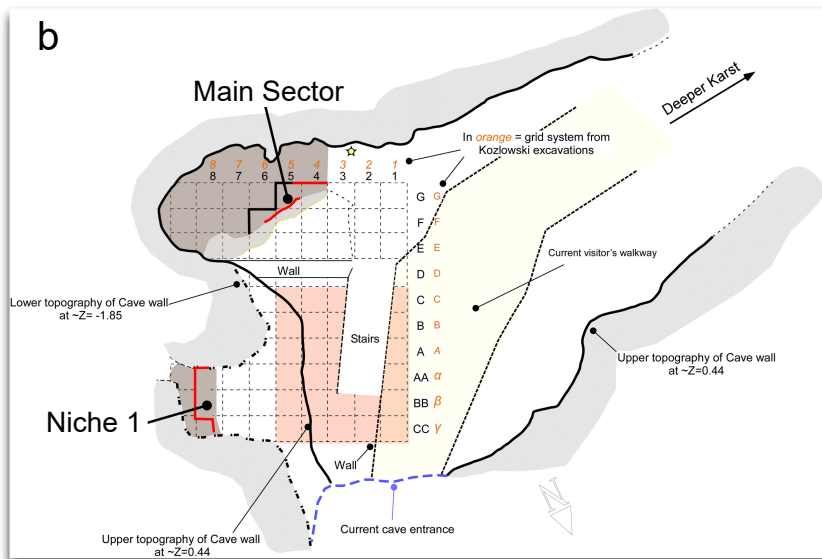
527 **Tables**

528

529 **Table 1.** Previously published radiocarbon dates on material excavated from Bacho Kiro Cave from 1971-
530 1975.

Layer	Sample type	AMS lab number	¹⁴ C age	1σ error (years)	Reference
7	Charcoal	OxA-3181	32,200	780	⁸
6a/7	Bone	Ly1102	29,150	950	^{2,15}
6b	Charcoal	OxA-3182	33,300	820	⁸
6b	Bone (no. 972)	GrN-7569	32,700	300	²
11	Charcoal from hearth	GrN-7545	>43,000		²
11	Bone	OxA-3213	38,500	1,700	⁸
11	Charcoal	OxA-3183	37,650	1,450	⁸
11	Tooth	OxA-3212	34,800	1,150	⁸
11a	Bone	OxA-3184	33,750	850	⁸
13	Bone (nos. 933 and 936)	GrN-7570	>47,000		²

531





b



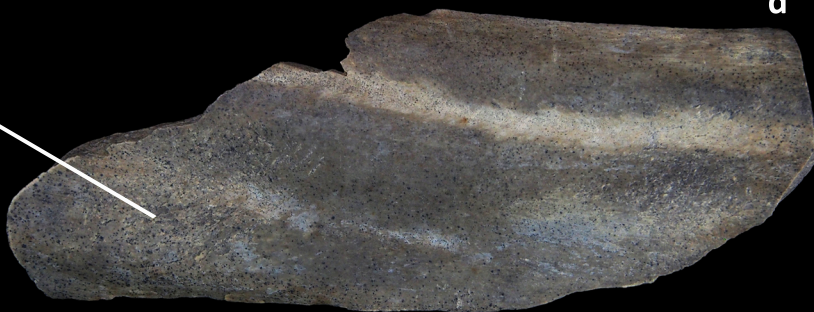
a



c



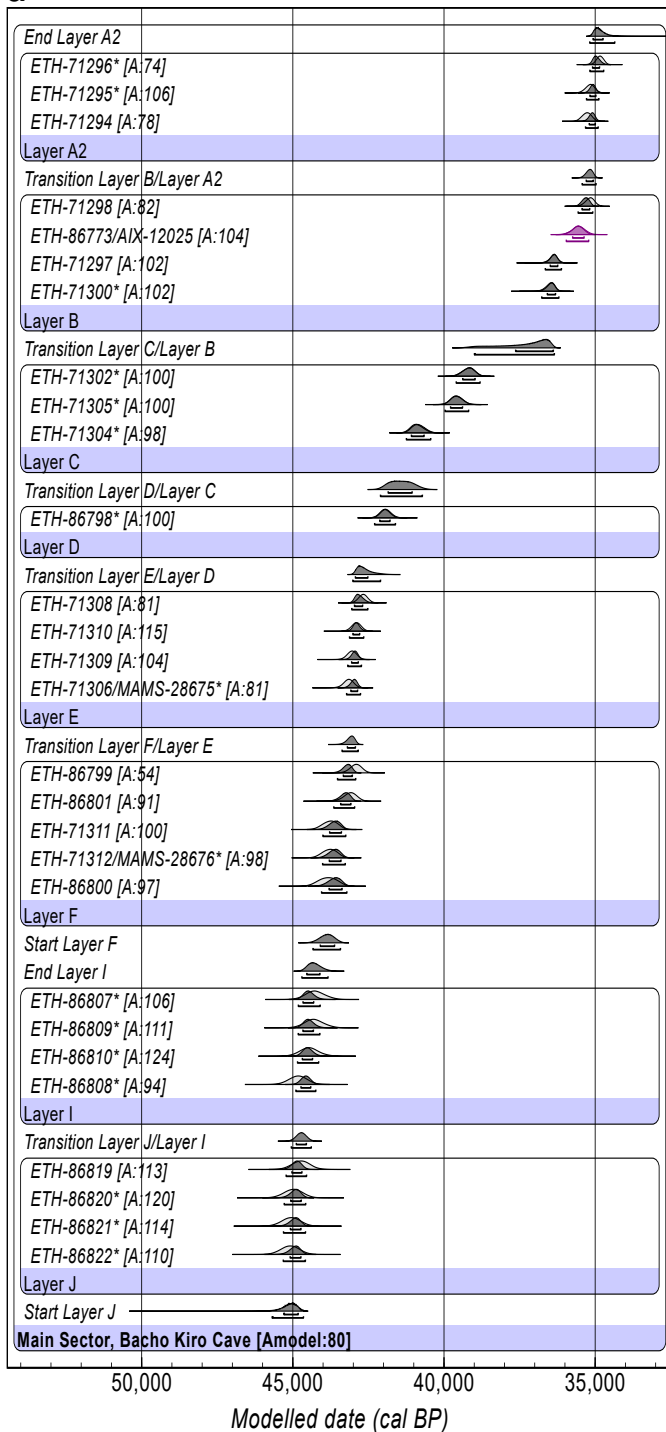
d



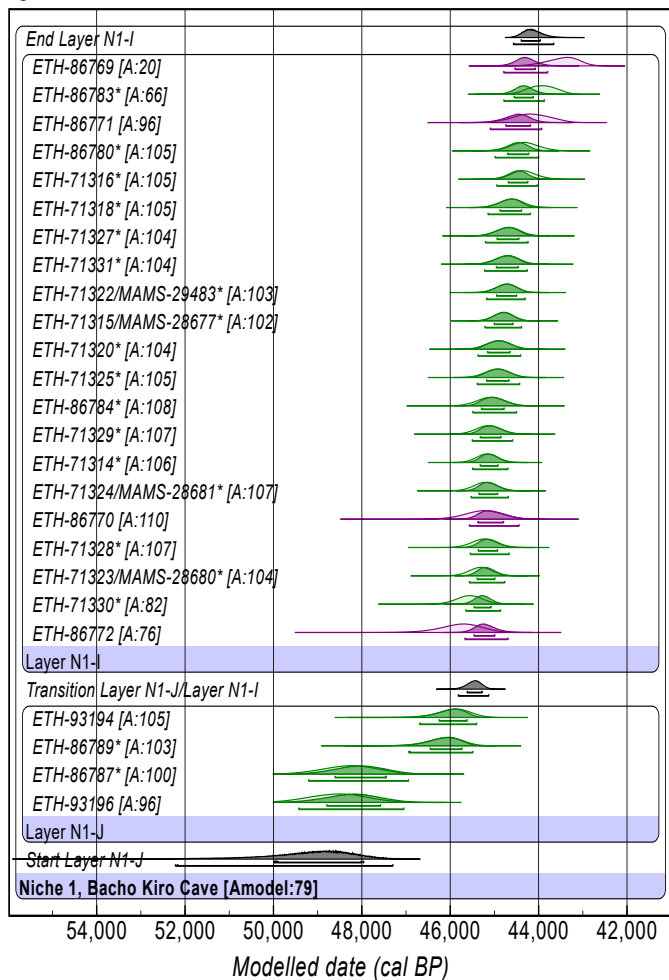
e



a



b



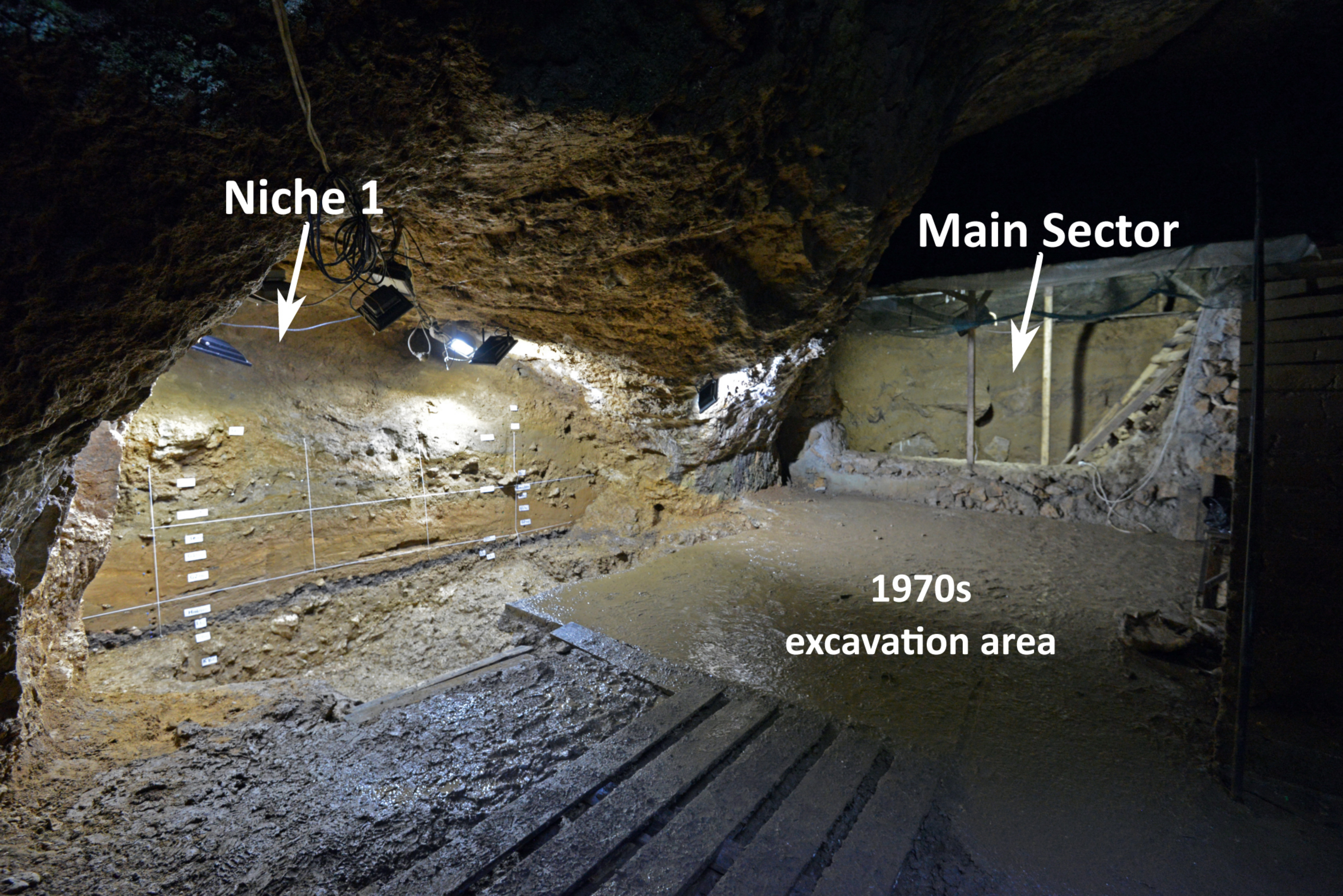
Niche 1



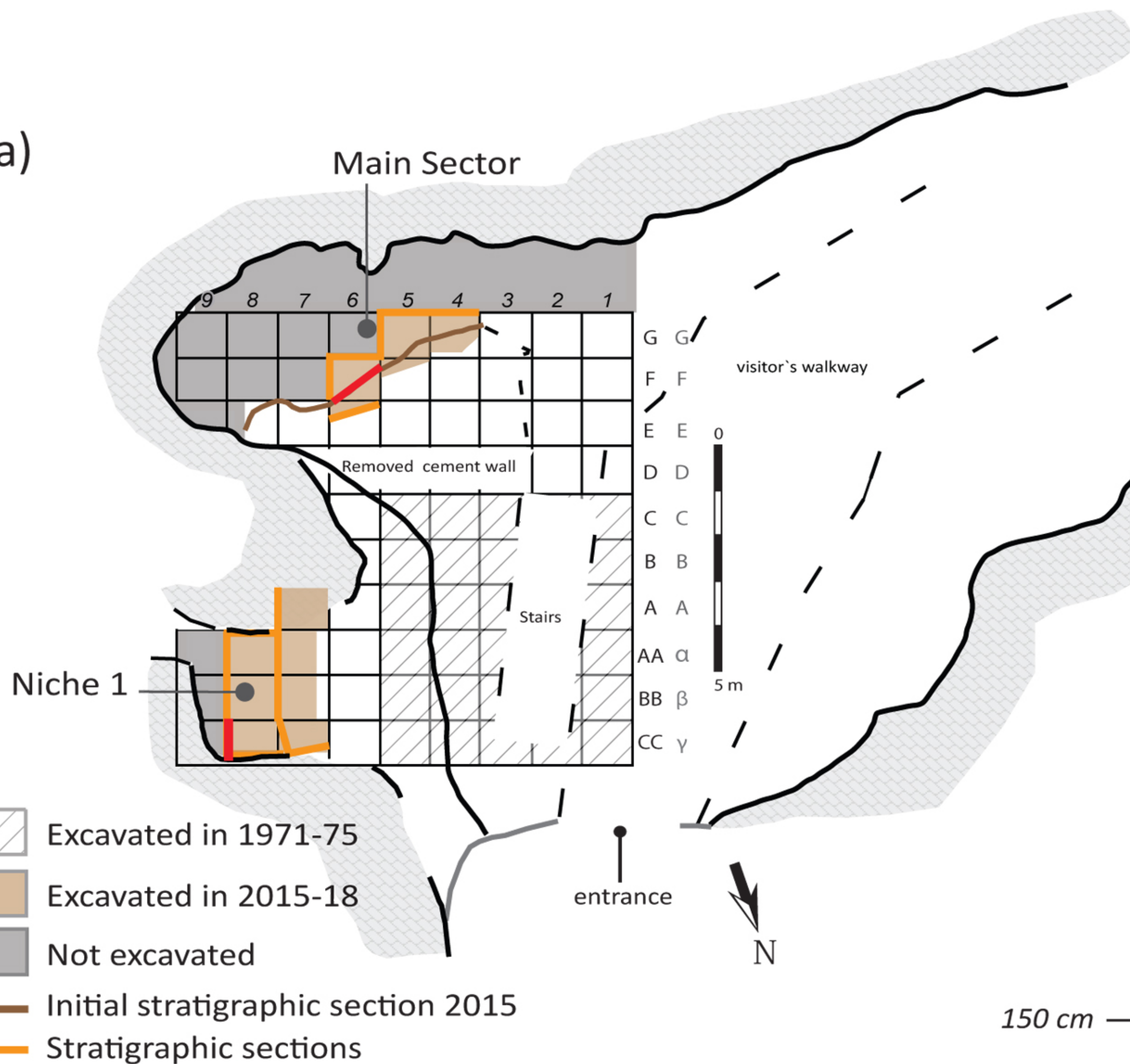
Main Sector



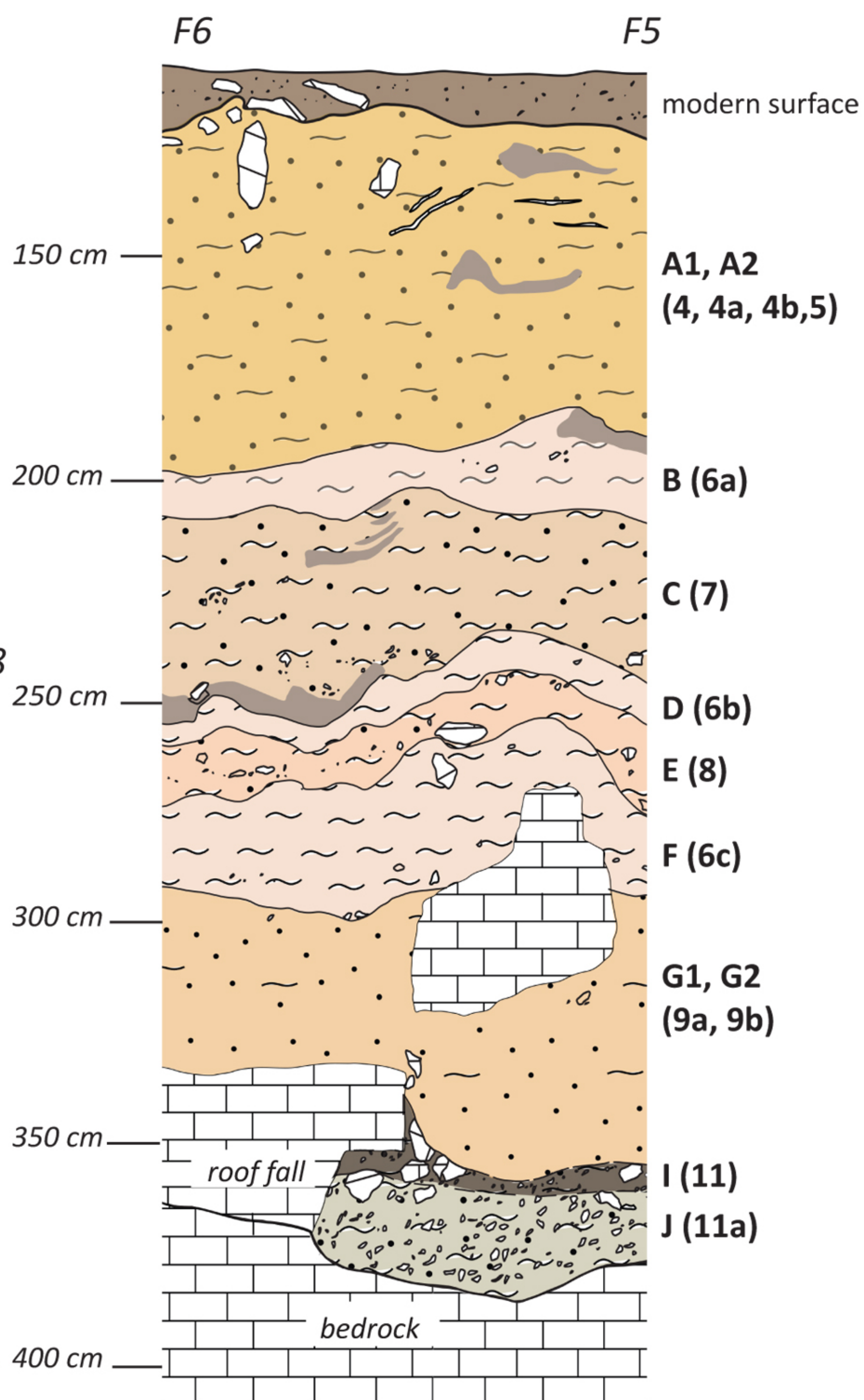
**1970s
excavation area**



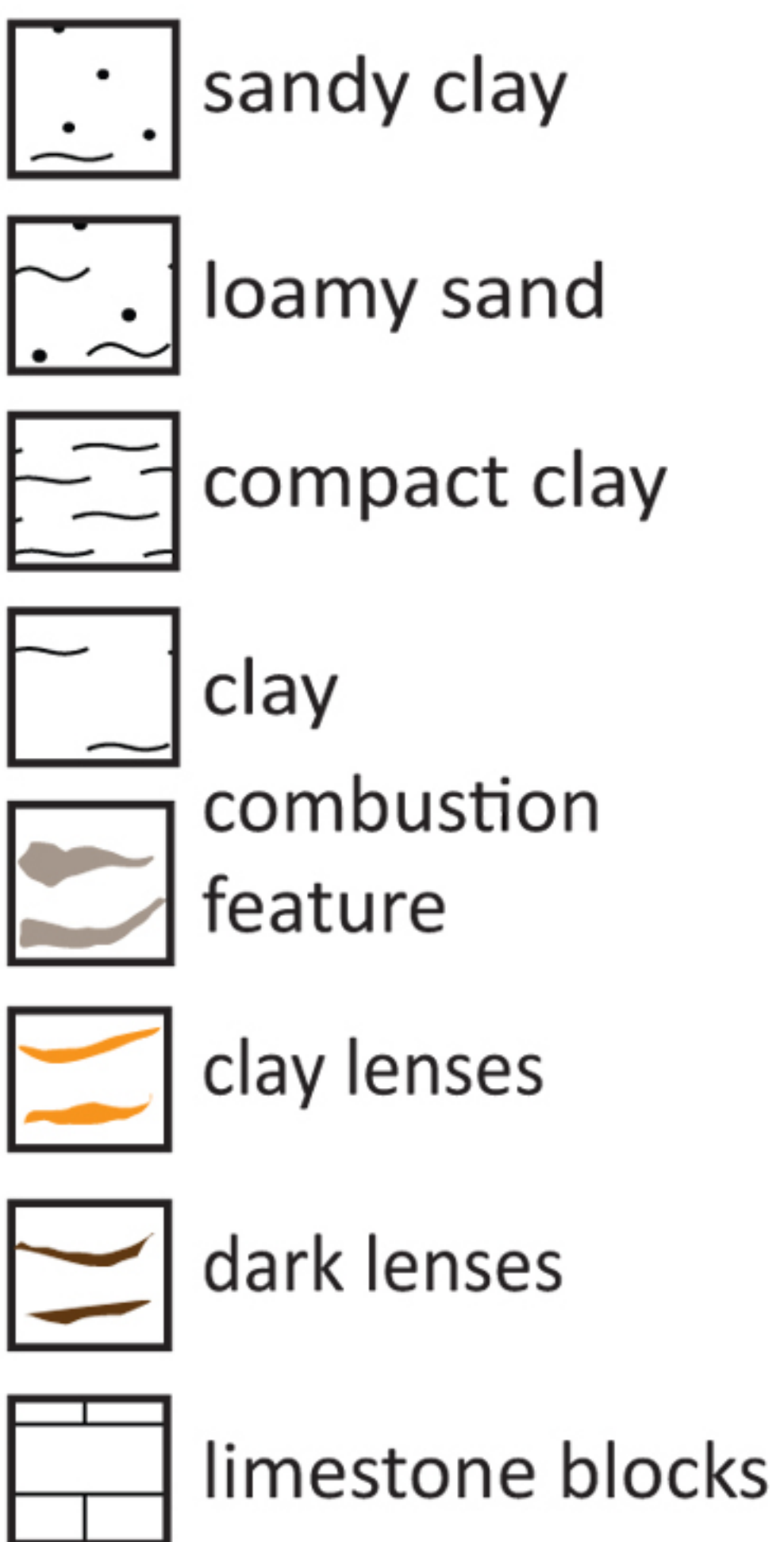
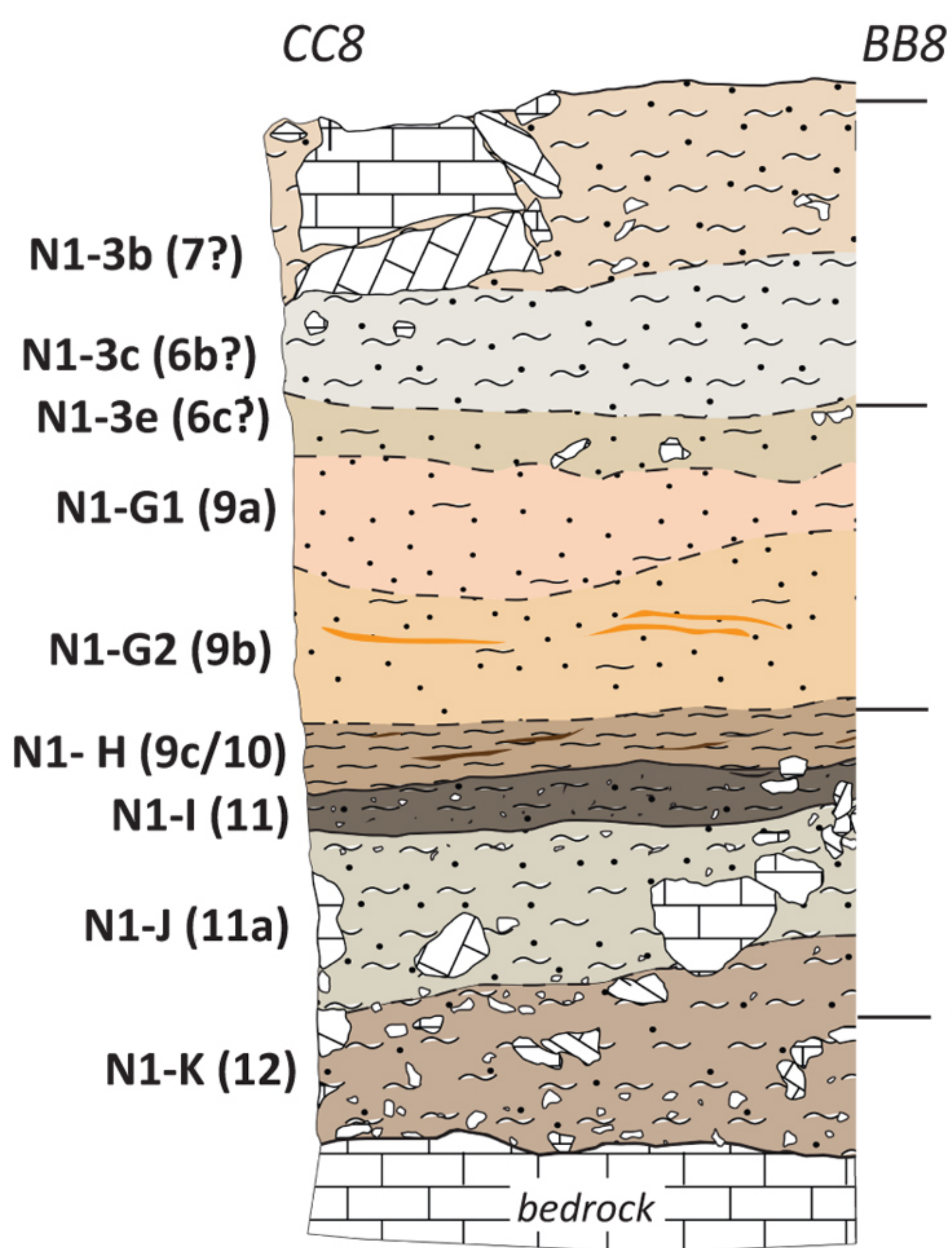
a)

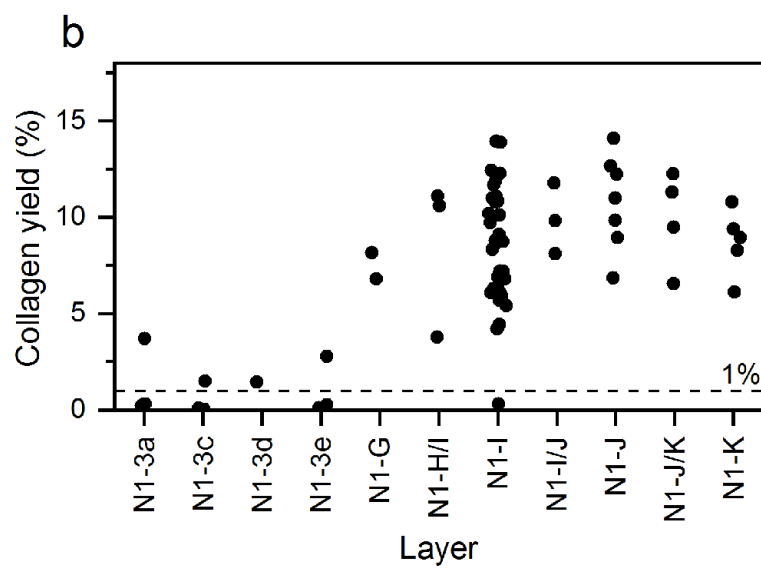
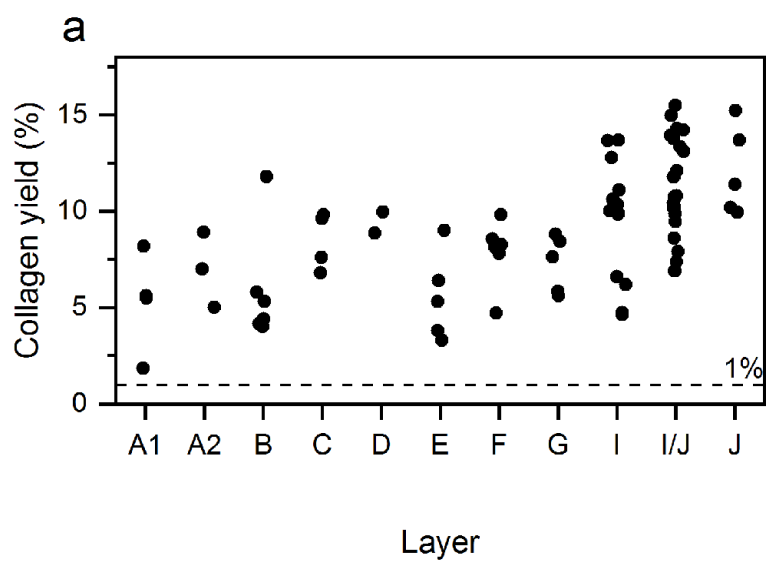


c) Main Sector

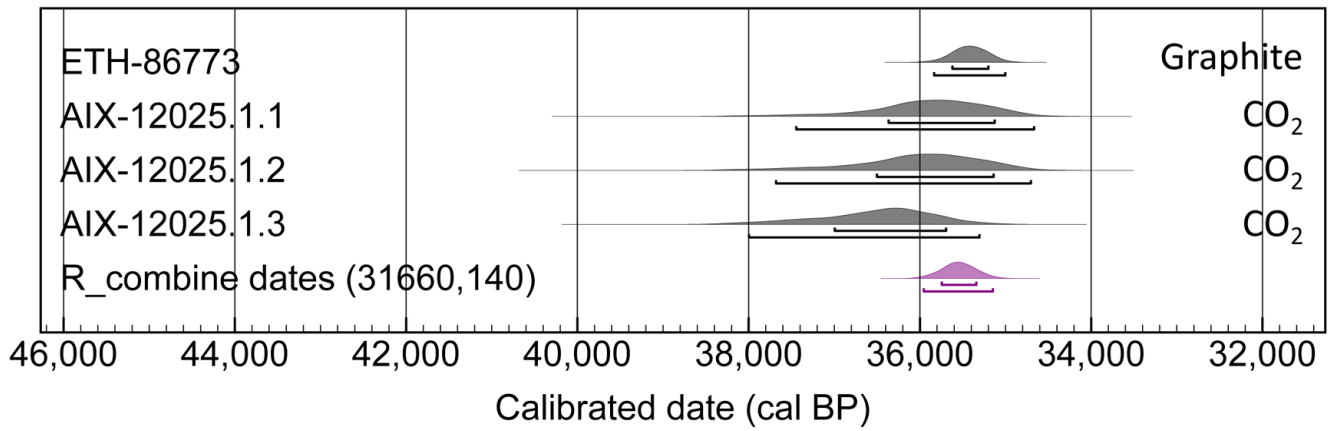


b) Niche 1





a



b

